

Supplementary Figures

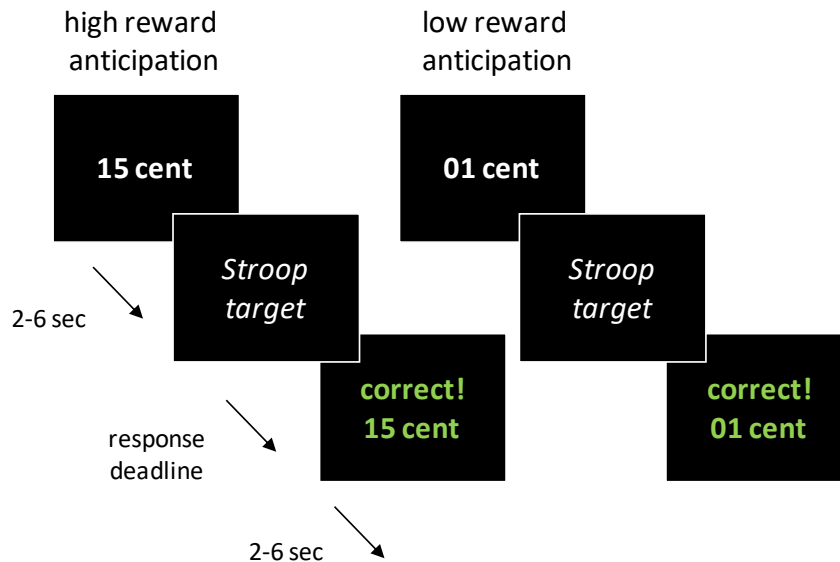


Figure S1. Reward anticipation task. Reward anticipation was assessed during fMRI in the context of a rewarded Stroop task. All trials began with a cue predicting high (15 cents) or low (1 cent) reward for correct performance on the target. The targets were arrow-word Stroop-like stimuli, with the word “LEFT” or “RIGHT” (relevant dimension) positioned in a left- or right-pointing arrow (irrelevant dimension). Participants responded to the target word using two button boxes, pressing the left button box with the left thumb or the right button box with the right thumb. The direction denoted by the word was either congruent or incongruent with the direction indicated by the arrow. Here, we focused our analyses on the reward cues (i.e. reward anticipation: high > low reward cues) preceding the targets. The task resembled a Stroop paradigm used previously [1], except that the ‘information cues’ were excluded from the current paradigm, the inter-stimulus intervals were greater (2–6 sec), and the participants received direct feedback on whether the response was correct (+ 1 or + 15 cent earned), incorrect (0 cent earned), or too

late (0 cent earned). Reward cues and target congruency were equally distributed across the 120 trials (duration of 20 min).

Two practice blocks preceded the actual experiment: one to familiarize the participants with the Stroop task (40 trials) and one to familiarize the participants with the actual task including the reward cues (40 trials). The practice blocks were used to set the initial response window in the next part of the experiment, which was the average response time (RT) for trials responded to correctly per trial type. In the main experiment, reward was obtained only when an answer was correct and occurred within this response window determined individually for each participant. The initial response windows were adapted throughout the main experiment: after a correct response that was on time, 10 ms was subtracted from the response window for that trial type, and after a response that was too late, 25 ms was added to the response window for that trial type. Hence, frequency of reward receipt did not vary with difficulty and was similar across participants. After every 30 trials, participants were informed about the total amount of reward obtained at that point in a 15 seconds break. The reward money (mean ADHD: 5.94 EUR, SD: 1.15 EUR; mean controls: 5.91 EUR, SD: 0.80 EUR; $t(85)=-0.1$, ns) was added to the participants' compensation.

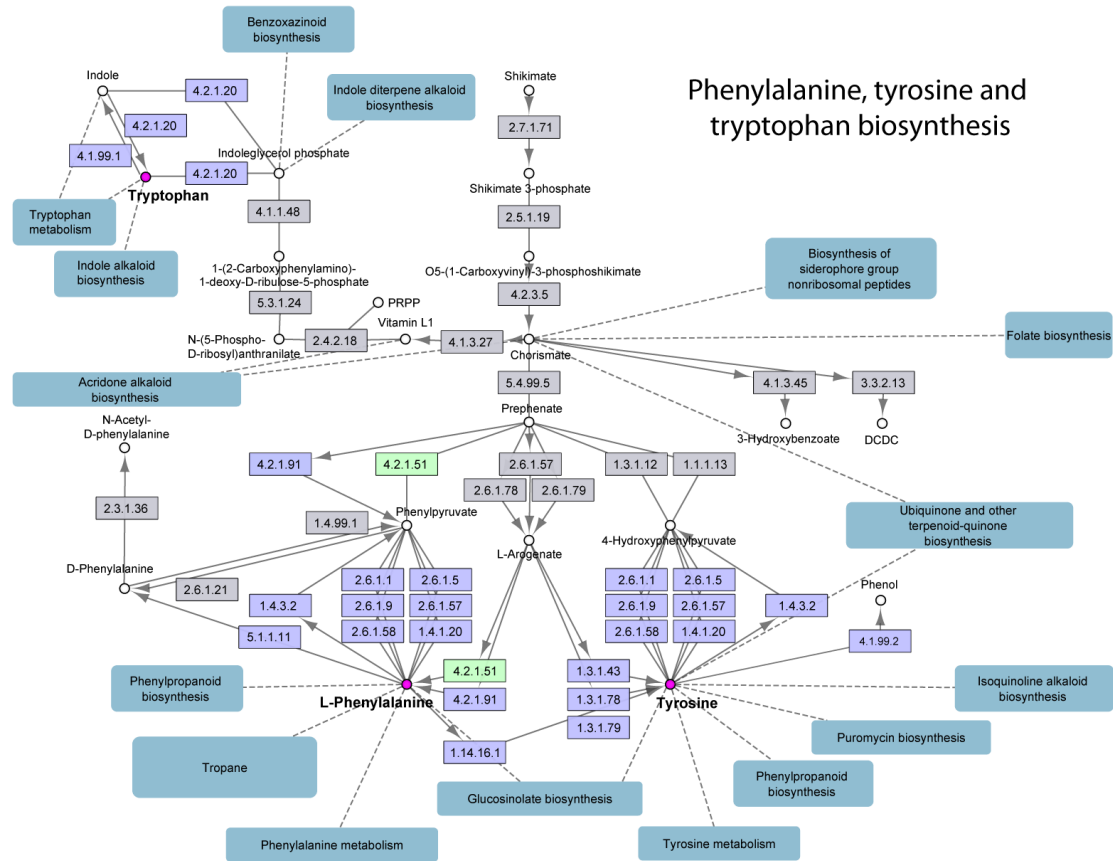


Figure S2. Monoamine precursor biosynthesis pathways. Visualization of a selection of the pathway maps of ‘Phenylalanine, tyrosine and tryptophan biosynthesis’ according to KEGG [2], created in Cytoscape [3] with the KEGGscape app [4] by combining various maps (ko00400, ko00360, ko00350 and ko00380) into one representation. Nodes represent compounds, pink nodes represent one of our compounds of interest: phenylalanine, tyrosine or tryptophan. Boxes represent enzyme functions/reactions, numbers shown inside are enzyme (EC) numbers. Boxes in blue correspond to candidates that were a priori selected for our function analysis by PICRUST, gray boxes were excluded from analysis. Arrows link the conversion of one compound to another, facilitated by an enzyme function/reaction. Dashed lines link compounds to other KEGG pathways.

The EC number with the green box (EC:4.2.1.51; K01713) represents the enzyme cyclohexadienyl dehydratase and is the one candidate reaction showing a diagnosis effect (see main [Figure 4](#)). Cyclohexadienyl dehydratase (also known as arogenate dehydratase) is involved in the synthesis of phenylalanine by two different routes: firstly, by directly converting arogenate to phenylalanine [5], secondly, by catalyzing the reaction of prephenate to phenylpyruvate [6]. Phenylpyruvate is then transaminated to phenylalanine by phenylpyruvate aminotransferase [7, 8].

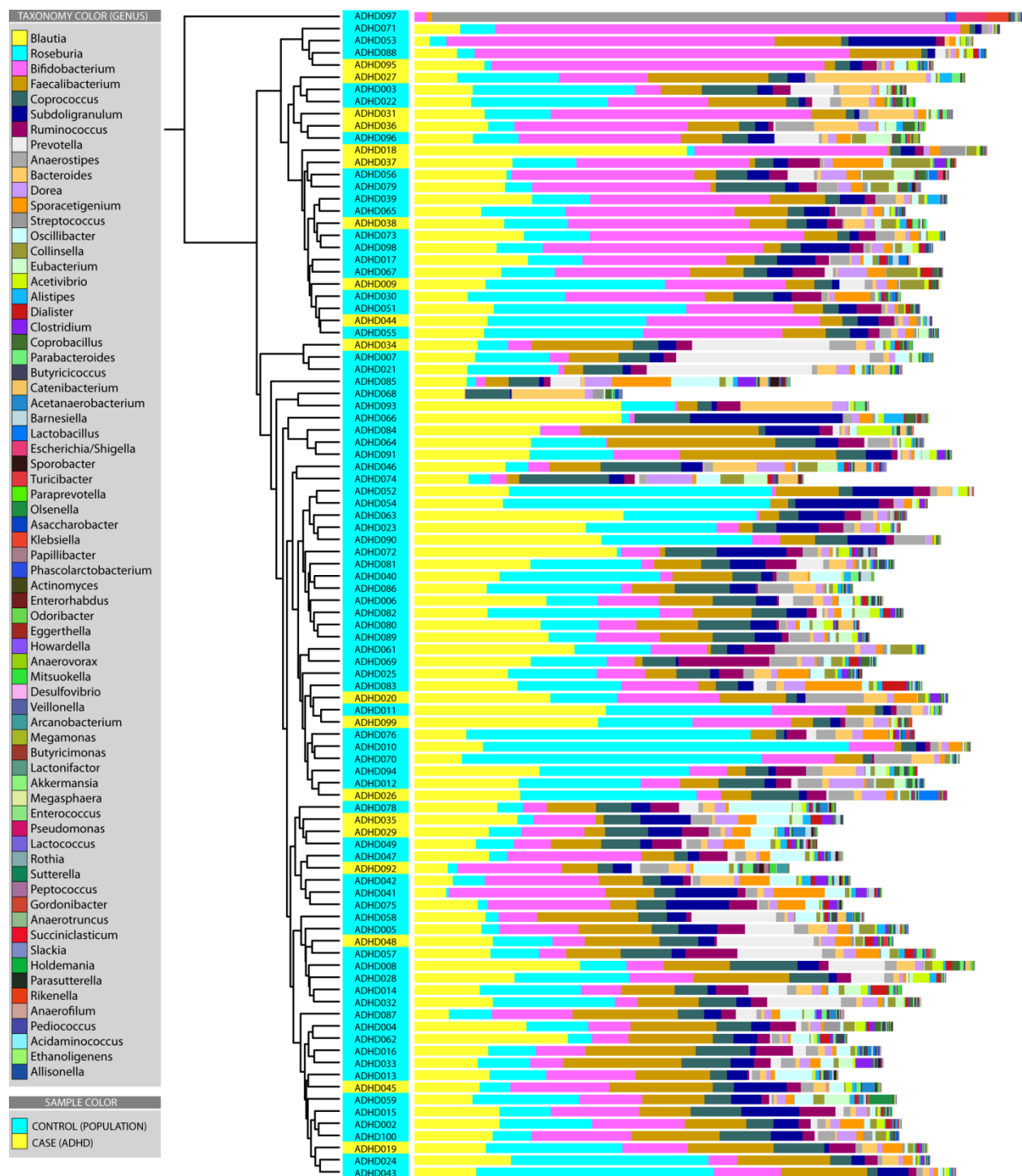


Figure S3. Intestinal microbiome composition. Clustering of 96 samples based on intestinal microbial composition on the genus level: 77 controls (population; in blue) and 19 cases (ADHD; in yellow). The composition is displayed as absolute abundance, which is the number of reads assigned to a genus.

Color bars represent absolute abundance of these bacterial genera as determined by 454 pyrosequencing. Hierarchical UPGMA clustering (Unweighted Pair Group Method with Arithmetic Mean) was performed with weighed UniFrac as distance measure, as implemented in QIIME 1.2. The figure was generated with the interactive tree of life (iTOL) program [9].

References Supplementary Figures

1. Aarts, E., et al., *Dopamine and the cognitive downside of a promised bonus*. Psychol Sci, 2014. **25**(4): p. 1003-9.
2. Kanehisa, M. and S. Goto, *KEGG: kyoto encyclopedia of genes and genomes*. Nucleic Acids Res, 2000. **28**(1): p. 27-30.
3. Shannon, P., et al., *Cytoscape: a software environment for integrated models of biomolecular interaction networks*. Genome Res, 2003. **13**(11): p. 2498-504.
4. Nishida, K., et al., *KEGGscape: a Cytoscape app for pathway data integration*. F1000Res, 2014. **3**: p. 144.
5. Fischer, R. and R. Jensen, *Arogenate dehydratase*. Methods Enzymol, 1987. **142**: p. 495-502.
6. Cotton, R.G. and F. Gibson, *The Biosynthesis of Phenylalanine and Tyrosine; Enzymes Converting Chorismic Acid into Prephenic Acid and Their Relationships to Prephenate Dehydratase and Prephenate Dehydrogenase*. Biochim Biophys Acta, 1965. **100**: p. 76-88.
7. Obmolova, G., et al., *Preliminary crystallographic study of cyclohexadienyl dehydratase from Pseudomonas aeruginosa*. J Mol Biol, 1993. **232**(3): p. 992-4.
8. Yoo, H., et al., *An alternative pathway contributes to phenylalanine biosynthesis in plants via a cytosolic tyrosine:phenylpyruvate aminotransferase*. Nat Commun, 2013. **4**: p. 2833.
9. Letunic, I. and P. Bork, *Interactive Tree Of Life (iTOL): an online tool for phylogenetic tree display and annotation*. Bioinformatics, 2007. **23**(1): p. 127-8.